

The Proper Motion of Sgr A*: II. The Mass of Sgr A*

M. J. Reid

Harvard-Smithsonian Center for Astrophysics, Cambridge, MA 02138

mreid@cfa.harvard.edu

A. Brunthaler

*Max-Planck-Institut für Radioastronomie, Auf dem Hügel 69, D-53121 Bonn, Germany and
Joint Institute for VLBI in Europe, Postbus 2, 7990 AA Dwingeloo, The Netherlands*

brunthal@jive.nl

ABSTRACT

We report measurements with the VLBA of the position of Sgr A* with respect to two extragalactic radio sources over a period of eight years. The apparent proper motion of Sgr A* relative to J1745–283 is 6.379 ± 0.024 mas y^{-1} along a position angle of 209.60 ± 0.18 degrees, almost entirely in the plane of the Galaxy. The effects of the orbit of the Sun around the Galactic center can account for this motion, and the residual proper motion of Sgr A* perpendicular to the plane of the Galaxy is -0.4 ± 0.9 km s^{-1} . A maximum-likelihood analysis of the motion expected for a massive object within the observed Galactic center stellar cluster indicates that Sgr A* contains more than about 10% of the $\approx 4 \times 10^6 M_{\odot}$ deduced from stellar orbits. The intrinsic size of Sgr A*, as measured by several investigators, is less than 1 AU, and the implied mass density of $\sim 10^{22} M_{\odot} \text{pc}^{-3}$ is within about three orders of magnitude of a comparable super-massive black hole within its Schwarzschild radius. Our observations provide the first direct evidence that a compact radiative source at the center of a galaxy contains of order $10^6 M_{\odot}$ and provides overwhelming evidence that it is in the form of a super-massive black hole. Finally, the existence of “intermediate mass” black holes more massive than $\sim 10^4 M_{\odot}$ between roughly 10^3 and 10^5 AU from Sgr A* are excluded.

Subject headings: Individual Sources: Sgr A*; Black Holes; Galaxy: Center, Fundamental Parameters, Structure; Astrometry

1. Introduction

The case for a super-massive black hole at the center of the Galaxy is extremely strong. The proper motions, accelerations, and orbits of stars about a common gravitational center are now being determined to high accuracy at infrared wavelengths (Schödel et al. 2002, 2003; Ghez et al. 2003). A total mass of $\approx 4 \times 10^6 M_{\odot}$ ¹ is required within a radius of about 100 AU. These dramatic results are fully consistent with the theory that Sgr A* , the compact radio source at the Galactic center, is a super-massive black hole. But must this matter be contained in a super-massive black hole (SMBH) and must Sgr A* be this SMBH?

The association of the gravitational mass inferred from infrared observations with the radiative source, Sgr A*, is supported primarily by two arguments: 1) the very close correspondence (better than ≈ 10 mas or 80 AU in projection) between the focal positions of the stellar orbits (Schödel et al. 2002, 2003; Ghez et al. 2003) and the infrared position of Sgr A*(Menten et al. 1997; Reid et al. 2003), and 2) the very short dynamical lifetimes of any massive dark cluster that would be required were Sgr A* not to contain most of the mass (Maoz 1998). Both arguments, while very strong, are perhaps not yet overwhelmingly so for two reasons. Firstly, Sgr A* is exceedingly under-luminous for a SMBH; its bolometric luminosity of $\ll 10^{37} L_{\odot}$ (Serabyn et al. 1997) is sub-Eddington for even a $1 M_{\odot}$ system. Thus, for example, a single, radio-loud, X-ray binary could mimic the emission from Sgr A*. Secondly, the short dynamical cluster lifetime arguments are predicated on the evolution of an *isolated* dense cluster at the Galactic center. It is possible that a quasi-steady-state condition could occur, whereby stars that are lost from the cluster (eg, by “evaporation”) are replaced by others falling inward from outside the cluster. The possibility of such steady-state conditions has not been addressed. Regardless of the resolution of these issues, any independent test of whether or not super-massive black holes exist is very important.

If the compact radio source, Sgr A*, is indeed the gravitational source then it should be nearly at rest at the dynamical center of the Galaxy. Backer & Sramek (1999) and Reid, Readhead, Vermeulen, & Treuhaft (1999) present radio interferometric data showing that the apparent proper motion of Sgr A* , measured against extragalactic sources, is consistent with that expected from the effects of the orbit of the Sun around the Galactic center. Removing the effects of the Sun’s motion, both papers conclude that the intrinsic motion of

¹The amount of mass in the central 100 AU region has been estimated to be between about 3 and 4 million solar masses, depending on the method used. Statistical estimators applied to proper motions give central masses toward the lower end of this range, while fits to stellar orbits favor the higher end of the range (Schödel et al. 2003; Ghez et al. 2003). The 3-D motion of IRS 9 favors the higher end of this range (Reid et al. 2003), provided that it is bound to Sgr A*. Throughout this paper we adopt a total mass of 4 million solar masses.

Sgr A* in the Galaxy is less than $\approx 20 \text{ km s}^{-1}$.

This paper presents new results on the proper motion of Sgr A*. We show that Sgr A* is indeed nearly stationary at the Galactic center, providing a strong upper limit to the motion of Sgr A* out of the plane of the Galaxy. Simple and conservative analyses indicate that Sgr A* contains at least 10% of this mass. The mass density of Sgr A*, obtained by combining the lower limit to the mass directly tied to Sgr A* from this paper with the apparent size upper limits from VLBI observations (Rogers et al. 1994; Krichbaum et al. 1998; Doeleman et al. 2001; Bower et al. 2004) is so extreme that the case for a super-massive black hole becomes overwhelming.

2. Observations

Our observations using the National Radio Astronomy Observatory’s ² Very Long Baseline Array (VLBA) were conducted between 1995 and 2003. The results of the observations from 1995 through 1997 were reported by Reid et al. (1999, hereafter Paper I). The observations and analysis for the data from 1998 through 2003 were similar to those described in Paper I. Briefly, the observing sequence involved rapid switching between compact extragalactic sources, J1745–283 and J1748–291, and Sgr A*. Sources were changed every 15 seconds. We used Sgr A* as the *phase-reference* source, because it is considerably stronger than the background sources and could be detected on individual baselines with signal-to-noise ratios typically between 10 and 20 in the 7 seconds of available on-source time. We edited and calibrated data using standard tasks in the Astronomical Image Processing System (AIPS) designed for VLBA data.

As discussed in Paper I, the dominant sources of relative position uncertainty are small errors in the atmospheric model used by the VLBA correlator. For some of the epochs analyzed in Paper I, we were able to improve our relative position uncertainties by modeling simultaneously the differenced-phase data for the “J1745–283 minus Sgr A*” and “J1748–291 minus Sgr A*” source pairs and solving for a relative position shift for each source pair as well as a single vertical atmospheric delay error for each antenna. However, this procedure requires high signal-to-noise ratio data for both background sources for any given baseline within an integration time of ~ 10 min. Unfortunately, J1748–291 weakened considerably after 1997 and we could not use this calibration technique for most of our observations, resulting in increased positional uncertainties for the post 1997 data (except for the 2003

²The National Radio Astronomy Observatory is operated by Associated Universities Inc., under a cooperative agreement with the National Science Foundation.

data as discussed below).

For the 2003 observations, we developed an alternative calibration approach that involved measuring directly the vertical atmospheric delay errors before, during, and after the ≈ 5.5 hr tracks on the Galactic center sources. Following procedures commonly used for geodetic VLBI observations (Walker 2000), we observed about a dozen strong extragalactic radio sources from the International Celestial Reference Frame catalog (Ma et al. 1998) in rapid succession over a period of about 45 min. These data were taken at 43 GHz, with eight 8-MHz bands that spanned 470 MHz of bandwidth, and residual multi-band delays and fringe rates were calculated for all sources. These data were modeled as owing to a vertical atmospheric delay and delay-rate, as well as a clock offset and clock drift rate, at each antenna. Typical formal uncertainties in the estimates of the vertical atmospheric delays (expressed as excess path lengths) were 0.2 to 0.3 cm. Our solutions for atmospheric delay errors include an ionospheric contribution, expected to be about 0.3 cm of vertical path length, which affects the phase referenced data and should also be removed when we correct the data. We did not solve for baseline or Earth’s orientation and spin parameters, as the values used during correlation are sufficiently accurate so as not to contribute significantly to the atmospheric parameter estimates. Similarly, we carefully chose extragalactic sources whose positions are known to better than 1 mas, so as to avoid position errors contributing significantly to the residual delays and rates. We corrected for the effects of the errors in the atmospheric model of the correlator on the phase-referenced data using a version of the AIPS task CLCOR provided by L. Kogan of NRAO. The image quality improved, and the scatter in the positions of J1745–283, corrected in this manner, is consistent with single epoch uncertainties of better than about 0.1 mas in the each coordinate axis.

For data prior to 1998 the position used during correlation of Sgr A*, the phase-reference source, was inaccurate by ≈ 0.12 arcsec. For the 1998 and subsequent data, a better position for Sgr A* was used when correlating the data. In order to combine all data, we corrected the pre-1998 data for this change in position. This change involved two steps. The first order effect is a straightforward translation. Fitted position offsets were added to the original correlator positions; then the new (better) source position was subtracted, yielding new position offsets. A subtle second-order correction is then required. In the phase-referencing process, residual interferometer phase-shifts for the phase-reference source (owing to the 0.12 arcsec absolute position error for Sgr A*) are subtracted from the source to be phase-referenced (eg, J1745–283) and “interpreted” as a position shift *based on the position of this source*. Since, the two sources are not at the same position on the sky, this leads to a second-order correction whose magnitude is roughly $\Delta\theta_{\text{err}} \times \theta_{\text{separation}}$. For our case, $\Delta\theta_{\text{err}} = 0.12$ arcsec and $\theta_{\text{separation}} \approx 0.01$ radians, leading to an expected shift of ≈ 1 mas. We simulated correlator visibility phases for the 0.12 arcsec position error for Sgr A* and

fitted them for a position offset for J1745–283. This indicated that we needed to subtract a second-order position correction of $(-0.734, +0.051)$ mas, in the (E,N) directions, from the pre-1998 data for J1745–283. A similar correction for J1748–291 of $(-1.049, +2.162)$ mas was needed.

The data in Table 1 summarize our relative position measurements. We have made no correction for the parallax of Sgr A*, which would shift its position by ≤ 0.1 mas in each coordinate and would be nearly identical for all data except the epochs near 1999.8. The position offsets are given relative to Sgr A*, the phase reference source, even though it is Sgr A* that appears to move and not J1745–283 or J1748–291. Reversing the signs of the offsets, the positions on the sky of Sgr A*, relative to the the strongest background source, J1745–283, are plotted in Fig. 1. A weighted least-squares fit to the easterly and northerly positions versus time (dashed line in Fig. 1) produces a track on the sky that, while close to, clearly deviates from the Galactic plane. This can be explained by the known component of the Solar Motion perpendicular to the Galactic plane.

The best-fit apparent motion of Sgr A* relative to J1745–283 is given in Table 2. The uncertainties in Table 2 include estimates of systematic effects, dominated by small residual errors in modeling atmospheric delays. Assuming that J1745–283 is sufficiently distant that it has negligible intrinsic angular motion, Sgr A*'s apparent motion is -3.151 ± 0.018 and -5.547 ± 0.026 mas y^{-1} in the easterly and northerly directions, respectively.

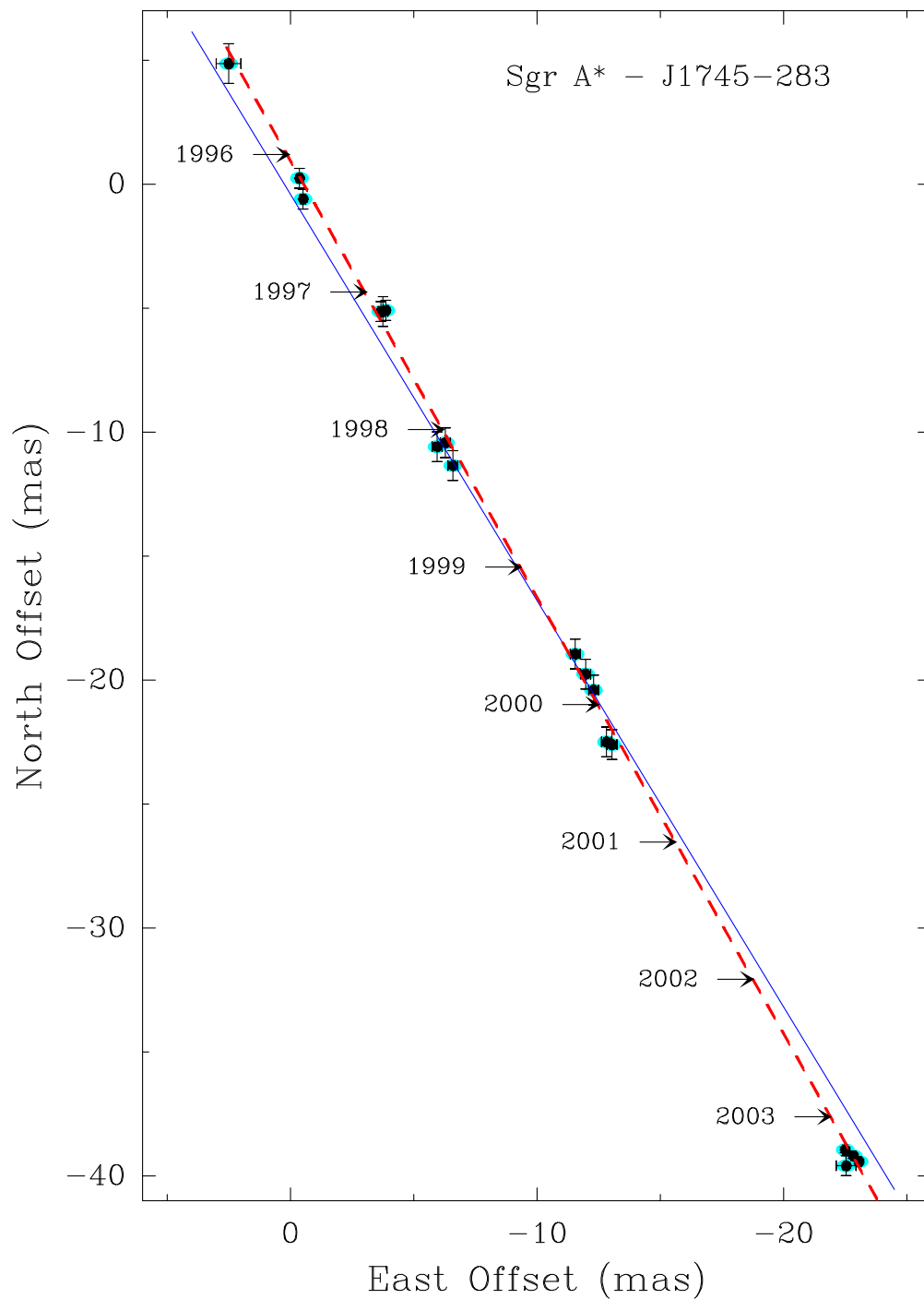


Fig. 1.— Position residuals of Sgr A* relative to J1745-283 on the plane of the sky. Each measurement is indicated with an ellipse, approximating the apparent scatter-broadened size of Sgr A* at 43 GHz and 1σ error bars, which include estimates of systematic uncertainties. The dashed line is the variance-weighted best-fit proper motion, and the solid line gives the orientation of the Galactic plane, which is tilted by 31.40° east of north in J2000 coordinates (see Appendix).

Table 1. Residual Position Offsets Relative to Sgr A*

Source	Date of Observation	East Offset (mas)	North Offset (mas)	ℓ^{II} Offset (mas)	b^{II} Offset (mas)
J1745–283	1995.178	-2.50 ± 0.5	-4.87 ± 0.8	-5.46 ± 0.63	-0.40 ± 0.63
	1996.221	0.37 ± 0.1	-0.25 ± 0.4	-0.02 ± 0.20	-0.44 ± 0.20
	1996.252	0.52 ± 0.1	0.59 ± 0.4	0.77 ± 0.20	-0.14 ± 0.20
	1997.211	3.67 ± 0.1	5.13 ± 0.4	6.29 ± 0.20	-0.46 ± 0.20
	1997.241	3.87 ± 0.1	5.08 ± 0.4	6.35 ± 0.20	-0.66 ± 0.20
	1997.241	3.76 ± 0.2	5.13 ± 0.6	6.33 ± 0.35	-0.54 ± 0.35
	1998.202	5.95 ± 0.2	10.58 ± 0.6	12.13 ± 0.35	0.43 ± 0.35
	1998.219	6.29 ± 0.2	10.42 ± 0.6	12.17 ± 0.35	0.06 ± 0.35
	1998.230	6.59 ± 0.2	11.34 ± 0.6	13.11 ± 0.35	0.28 ± 0.35
	1999.791	11.55 ± 0.2	18.95 ± 0.6	22.19 ± 0.35	0.01 ± 0.35
	1999.799	12.29 ± 0.2	20.40 ± 0.6	23.82 ± 0.35	0.13 ± 0.35
	1999.805	11.97 ± 0.2	19.75 ± 0.6	23.10 ± 0.35	0.07 ± 0.35
	2000.232	13.04 ± 0.2	22.60 ± 0.6	26.08 ± 0.35	0.64 ± 0.35
	2000.238	12.82 ± 0.2	22.49 ± 0.6	25.88 ± 0.35	0.77 ± 0.35
	2003.264	22.51 ± 0.1	38.94 ± 0.2	44.96 ± 0.14	1.08 ± 0.14
	2003.318	22.84 ± 0.1	39.18 ± 0.2	45.34 ± 0.14	0.92 ± 0.14
	2003.339	22.54 ± 0.4	39.59 ± 0.4	45.53 ± 0.40	1.38 ± 0.40
	2003.353	23.06 ± 0.1	39.41 ± 0.2	45.66 ± 0.14	0.85 ± 0.14
	J1748–291	1996.221	1.04 ± 0.2	-2.09 ± 0.6	-1.24 ± 0.35
1996.252		1.06 ± 0.2	-2.18 ± 0.6	-1.31 ± 0.35	-2.04 ± 0.35
1997.211		4.53 ± 0.2	2.76 ± 0.6	4.72 ± 0.35	-2.43 ± 0.35
1997.241		4.62 ± 0.2	2.44 ± 0.6	4.49 ± 0.35	-2.68 ± 0.35
1998.202		7.65 ± 0.2	8.34 ± 0.6	11.10 ± 0.35	-2.19 ± 0.35
1998.230		7.65 ± 0.2	8.10 ± 0.6	10.90 ± 0.35	-2.31 ± 0.35
1999.791		12.87 ± 0.2	17.79 ± 0.6	21.89 ± 0.35	-1.72 ± 0.35
1999.799		12.64 ± 0.2	17.18 ± 0.6	21.25 ± 0.35	-1.84 ± 0.35
1999.805		12.94 ± 0.2	17.84 ± 0.6	21.97 ± 0.35	-1.76 ± 0.35
2000.232		13.98 ± 0.2	20.05 ± 0.6	24.40 ± 0.35	-1.48 ± 0.35
2000.238		14.13 ± 0.2	20.54 ± 0.6	24.90 ± 0.35	-1.36 ± 0.35
2000.246		13.95 ± 0.2	19.90 ± 0.6	24.25 ± 0.35	-1.54 ± 0.35
2003.264		23.42 ± 0.2	37.89 ± 0.6	44.54 ± 0.35	-0.25 ± 0.35
2003.318		23.96 ± 0.2	37.17 ± 0.6	44.20 ± 0.35	-1.09 ± 0.35

One potential source of relative positional error is structural variability of the radio sources. Since both extragalactic sources and Sgr A* could have a core-jet structure, we could, in principle, be measuring the centroid of a stationary core and a moving component of an inner-jet. These effects, however, are likely quite small as we are observing at a very high frequency, where 1) stationary cores usually are dominant and 2) time variations are usually rapid ($\ll 8$ y) and will “average out.” Indeed, all of our images are consistent with a point-source, broadened by interstellar scattering. Finally, the results of VLBA observations by Bower, Backer, & Sramek (2001) at 2.3, 5.0 and 8.4 GHz, when extrapolated to 43 GHz, suggest that source structure is not likely to significantly affect our relative source positions.

Because we have two reference sources, which should have independent structures and variations, we can place an observational upper limit on the magnitude of position wander caused by source structure changes or any other effects, such as gravitational deflections by intervening stars in the Galaxy (Hosokawa et al. 2002). We determined relative positions between the two calibration sources and plot these in Fig. 2 in the sense “J1748–291 minus J1745–283.” The best-fit motions are -0.052 ± 0.035 and -0.126 ± 0.061 mas y^{-1} in the easterly and northerly directions, respectively, as indicated by the dashed lines. Were either or both of these Galactic sources, a much larger relative motion (> 1 mas y^{-1}) would be expected. Clearly both are extragalactic.

The *uncertainty* in the relative motion of J1748–291 with respect to J1745–283 is significantly larger than for the motion of Sgr A* with respect to J1745–283, because 1) it involves differencing two measured relative positions, 2) the angular separation of the two background sources (≈ 1.0 deg) is greater than between Sgr A* and either of the background sources (≈ 0.7 deg), which increases sensitivity to systematic errors, and 3) J1748–291 is the weakest of the three sources and not detected at all epochs. The background sources display little if any motion relative to each other. The easterly motion of J1748–291 relative to J1745–283 is entirely consistent with measurement errors, while the measured northerly motion is approximately twice the 1σ error. Were structural variability to contribute to our measurement uncertainty, it likely is comparable to or less than our 1σ uncertainties.

3. Results

The apparent motion of Sgr A* with respect to background radio sources can be used to estimate the rotation of the Galaxy and any peculiar motion of the super-massive black hole candidate Sgr A*. The apparent motion in the plane of the Galaxy should be dominated by the effects of the orbit of the Sun around the Galactic Center, while the motion out of the plane should contain only small terms from the Z-component of the Solar Motion and a

Table 1—Continued

Source	Date of Observation	East Offset (mas)	North Offset (mas)	ℓ^{II} Offset (mas)	b^{II} Offset (mas)
--------	------------------------	----------------------	-----------------------	-----------------------------	--------------------------

Note. — Position offsets are relative to Sgr A*, after removing the ≈ 0.7 degree differences of the background sources. The coordinate offsets are relative to the following J2000 positions for Sgr A* (17 45 40.0409, $-29\ 00\ 28.118$), J1745–283 (17 45 52.4968, $-28\ 20\ 26.294$), and J1748–291 (17 48 45.6860, $-29\ 07\ 39.404$). The conversion to Galactic coordinates is discussed in the Appendix. The positions for epochs before 1998 have been corrected for the second-order effects of processing the phase-reference data from Sgr A* with J2000 coordinates of (17 45 40.0500, $-29\ 00\ 28.120$).

Table 2. Apparent Relative Motions

Source – Reference	Easterly Motion (mas y^{-1})	Northerly Motion (mas y^{-1})	ℓ^{II} Motion (mas y^{-1})	b^{II} Motion (mas y^{-1})
Sgr A* – J1745–283	-3.151 ± 0.018	-5.547 ± 0.026	-6.379 ± 0.026	-0.202 ± 0.019
J1748–291 – J1745–283...	-0.052 ± 0.035	-0.126 ± 0.061	-0.131 ± 0.060	-0.021 ± 0.037

Note. — Motions are from weighted least-squares fits to the data in Table 1. All results are in the J2000 coordinate system. Conversion of equatorial to Galactic coordinates in J2000 is discussed in the Appendix.

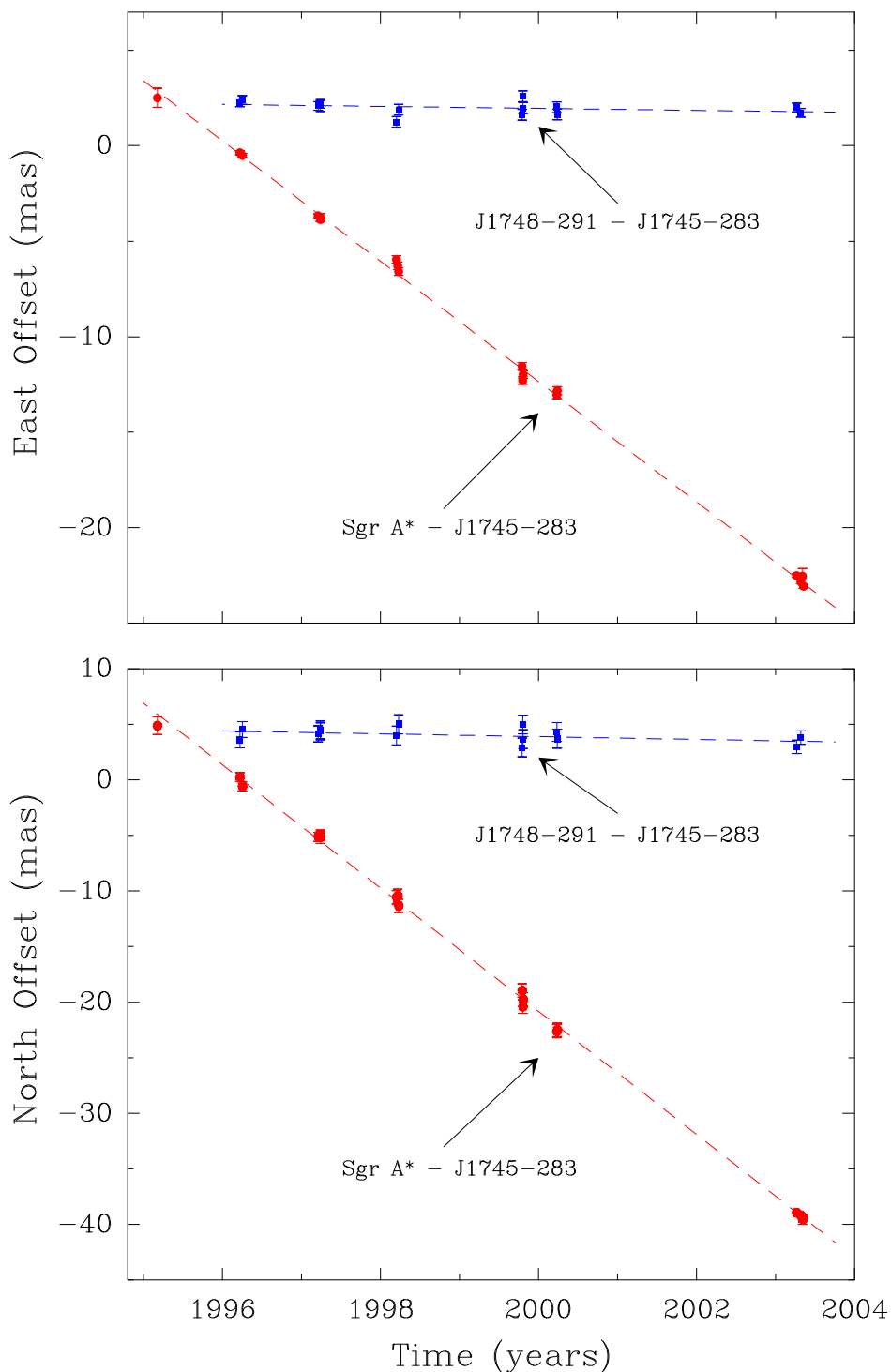


Fig. 2.— Position residuals of Sgr A* relative to J1745-283 and J1748-291 relative to J1745-283 toward the easterly (*top panel*) and northerly (*bottom panel*) directions. The J1748-291 positions are offset for clarity. Error bars are $\pm 1\sigma$ and include estimates of systematic effects. The position uncertainties are greater for J1748-291, owing partly to its weakness and its larger angular offset from J1745-283, compared to Sgr A*. The dashed lines are the variance-weighted best-fit proper motions. The position of J1748-291 relative to J1745-283 is constant within 2σ formal uncertainties and consistent with that expected for two extragalactic sources.

possible peculiar motion of Sgr A*. In the following subsections, we investigate the various components of the apparent velocity and acceleration of Sgr A*.

3.1. Motion of Sgr A* in the Plane of the Galaxy

It is clear from Fig. 1 that the apparent motion of Sgr A* is almost entirely in the Galactic plane. Thus, we convert the positions from equatorial to Galactic coordinates and determine motions in Galactic coordinates. (Because of the high accuracy of our observations, some pitfalls in the implementation of the equatorial to Galactic coordinate conversion (Lane 1979), and the need to transfer the IAU–defined plane from B1950 to J2000 coordinates, we document the procedures involved in the Appendix.) Fig. 4 is a plot the position of Sgr A* relative to J1745–283 in Galactic coordinates. Variance-weighted least-squares fits of straight lines to these data are indicated by dashed lines. The apparent motion of Sgr A* is -6.379 ± 0.026 and -0.202 ± 0.019 mas y^{-1} in Galactic longitude and latitude, respectively.

Assuming a distance to the Galactic center (R_0) of 8.0 ± 0.5 kpc (Reid 1993), the apparent angular motion of Sgr A* in the plane of the Galaxy translates to -241 ± 15 km s^{-1} . The uncertainty from measurement error alone is only 1 km s^{-1} , and the quoted value is dominated by the 0.5 kpc uncertainty in R_0 . Provided that the peculiar motion of Sgr A* is small (see §3.2), this corresponds to the reflex of true orbital motion of the Sun around the Galactic Center. This reflex motion can be parameterized as a combination of a circular orbit (i.e., of the LSR) and the deviation of the Sun from that circular orbit (the Solar Motion). The Solar Motion, determined from Hipparcos data by Dehnen & Binney (1998), is 5.25 ± 0.62 km s^{-1} in the direction of Galactic rotation. Removing this component of the Solar Motion from the *reflex* of the apparent motion of Sgr A* yields an estimate for Θ_0 of 236 ± 15 km s^{-1} . Note that other definitions and measurements of this component of the Solar Motion have resulted in somewhat greater values, eg, 12 km s^{-1} (Cox 2000), which if adopted would reduce our value of Θ_0 to 229 km s^{-1} . Should R_0 be determined independently to high accuracy, then our measurement of the apparent motion of Sgr A* would give Θ_0 with corresponding accuracy. Orbital solutions for stars near Sgr A* that combine proper motions and radial velocities have great potential to accomplish this (Eisenhauer et al. 2003; Ghez et al. 2003).

A direct comparison of our measurement of the *angular* rotation rate of the LSR at the Sun (Θ_0 / R_0) can be made with Hipparcos measurements based on motions of Cepheids. Feast & Whitelock (1997) conclude that the angular velocity of circular rotation at the Sun, Θ_0 / R_0 (= Oort’s A–B), is 27.19 ± 0.87 km s^{-1} kpc $^{-1}$ (218 ± 7 km s^{-1} for $R_0 = 8.0$ kpc). Our value of Θ_0 / R_0 , obtained by removing the Solar Motion in longitude from the

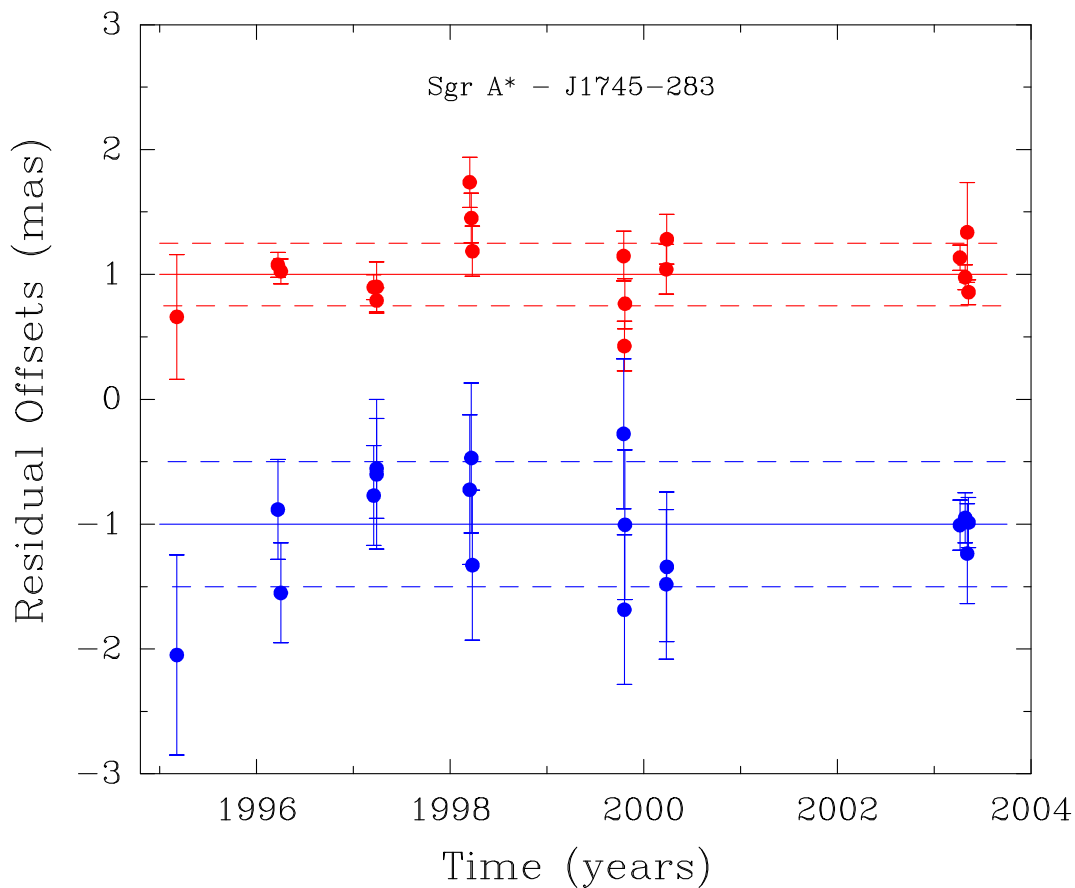


Fig. 3.— Residual offsets of Sgr A* relative to J1745–283 with best-fit motions removed. Easterly residuals are plotted above northerly residuals, shifted by +1 and –1 mas, respectively, for clarity. Solid lines indicate zero residual with respect to the best fitting motions shown in Fig. 2, and dashed lines indicate estimated limits for any short-period position excursions of Sgr A*. Data close in time (i.e., $\Delta t \approx 1$ week) appear slightly correlated, possibly owing to atmospheric systematics. Error bars are 1σ , including systematic effects of mis-modeled atmospheric delays.

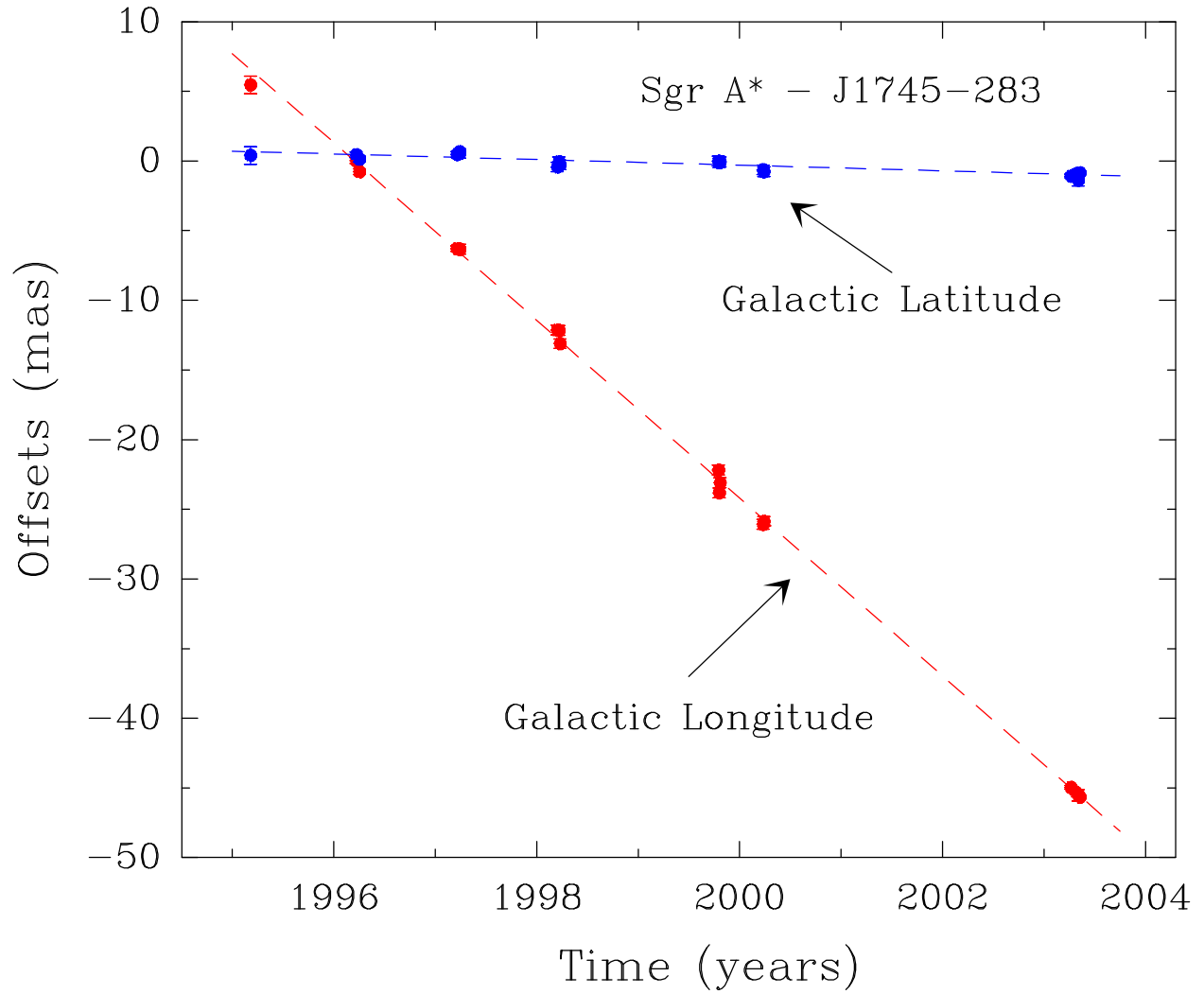


Fig. 4.— Position residuals of Sgr A* relative to J1745–283 in Galactic coordinates. Galactic longitude and latitude components are indicated along with their 1σ uncertainties. Dashed lines give the variance-weighted best-fit components of proper motion.

reflex of the motion of Sgr A* in longitude, is $29.45 \pm 0.15 \text{ km s}^{-1} \text{ kpc}^{-1}$. The difference between the VLBA and Hipparcos angular velocities is $2.26 \pm 0.9 \text{ km s}^{-1} \text{ kpc}^{-1}$; these measurements are marginally consistent. Neither measurements are sensitive to the value of R_0 , as it is primarily used only to remove the small contribution of the Solar Motion. Other measurements of Θ_0/R_0 , for example from proper motions of halo stars relative to galaxies by Kalirai et al. (2004), yield consistent values with slightly greater observational uncertainty.

Our value of Θ_0/R_0 is a true “global” measure of the angular rotation rate of the Galaxy, as opposed to those derived from Oort’s constants, which indirectly determine Θ_0 from the shear and vorticity in the velocity field of material in the solar neighborhood (Kerr & Lynden-Bell 1986). The small difference between the local (A–B) and global measures of Θ_0/R_0 suggests that local variations in Galactic dynamics ($d(\Theta/R)/dR$) are less than $\approx 3 \text{ km s}^{-1} \text{ kpc}^{-1}$.

We now estimate the peculiar motion of Sgr A* in the direction of Galactic rotation by subtracting the Hipparcos-based angular rotation rate of the Galaxy from the VLBA angular motions of Sgr A*. After removing the current best estimate of the motion of the Sun around the Galactic Center of $223 (218+5.25) \text{ km s}^{-1}$ (Feast & Whitelock 1997; Dehnen & Binney 1998) from our VLBA observation of 241 km s^{-1} , we find the peculiar motion of Sgr A* is $-18 \pm 7 \text{ km s}^{-1}$ toward positive Galactic longitude (see Table 3). This estimate of the “in-plane” motion of Sgr A* comes from differencing two *angular* motions. Since this difference is small, the uncertainty in R_0 does not strongly affect this component of the peculiar motion of Sgr A*. It is unclear at this time whether or not the estimate of this component of the peculiar motion of Sgr A* differs significantly from zero and, if so, if this indicates a difference between the global and local measures of the angular rotation rate of the Galaxy or a much larger peculiar motion for Sgr A* in the plane of the Galaxy compared to out of the plane (see §3.2).

Table 3 summarizes the apparent motion of Sgr A* in Galactic coordinates with various known sources of motion removed. Clearly, these results are of great interest in regard to the structure and kinematics of the Galaxy and will be the subject of a later paper.

3.2. Motion of Sgr A* out of the Plane of the Galaxy

Whereas the orbital motion of the Sun (around the Galactic Center) complicates estimates of the “in-plane” component of the peculiar motion of Sgr A*, motions out of the plane are simpler to interpret. One needs only to subtract the small Z-component of the

Table 3. Sgr A*’s Motion in Galactic Coordinates^a

Description	ℓ^{II} (km s ⁻¹)	b^{II} (km s ⁻¹)
Observed Sgr A* motion	-241 ± 15	-7.6 ± 0.7
Effects of Solar Motion ^b removed	-236 ± 15	-0.4 ± 0.8
Effects of Galactic Rotation ^c removed	-18 ± 7	-0.4 ± 0.9

^aMotions are for Sgr A* relative to J1745–283 from fitting results in Table 2. Speeds assume $R_0 = 8.0 \pm 0.5$ kpc (Reid 1993). Quoted uncertainties are 1σ and include measurement uncertainty and an angular-to-linear motion scaling error from the uncertainty in R_0 .

^bAdopted Solar Motion with respect to a circular orbit is 5.25 ± 0.62 km s⁻¹ in ℓ^{II} and 7.17 ± 0.38 km s⁻¹ in b^{II} (Dehnen & Binney 1998).

^cAdopted circular rotation of 27.19 ± 0.87 km s⁻¹ kpc⁻¹ (Feast & Whitelock 1997) removed from our measured angular rotation rate of -29.45 ± 0.15 km s⁻¹ kpc⁻¹ (after correction for the Solar Motion) and then multiplied by $R_0 = 8.0$ kpc. The quoted uncertainty is dominated by measurement uncertainties for the adopted circular rotation of the Galaxy, scaled by R_0 . The 0.1 degree uncertainty in the tilt of the Galactic pole (Blaauw et al. 1960) causes the slight increase in the uncertainty in the b -direction.

Solar Motion from the observed motion of Sgr A* to estimate the out-of-plane component of the peculiar motion of Sgr A*. Using stars within about 0.1 kpc of the Sun and measured by Hipparcos, Dehnen & Binney (1998) find the Z-component for the Solar Motion to be $7.17 \pm 0.38 \text{ km s}^{-1}$. Other determinations of the Z-component of the Solar Motion, eg, $7.61 \pm 0.64 \text{ km s}^{-1}$ for stars with distances out to a few kpc by Feast & Whitelock (1997), are generally in agreement with the result of Dehnen & Binney (1998), but have greater uncertainties. Thus, we adopt the Dehnen & Binney (1998) value in this paper. The motion of Sgr A* in Galactic latitude, shown in Fig. 4, is re-plotted with an expanded scale in Fig. 5. The dashed line in the figure is a weighted least-squares fit to the data. The fitted slope of $-0.202 \pm 0.019 \text{ mas y}^{-1}$, or $-7.6 \pm 0.7 \text{ km s}^{-1}$ for $R_0 = 8.0 \text{ kpc}$, agrees almost exactly with the reflex of the Solar Motion out of the Galactic plane. Allowing for a 0.1 degree uncertainty in the tilt of the Galactic pole (Blaauw et al. 1960) increases slightly the uncertainty in the out of plane motion from 0.7 to 0.8 km s^{-1} . Subtracting $-7.17 \pm 0.38 \text{ km s}^{-1}$ from our measured apparent motion of Sgr A* out of the plane of the Galaxy, we estimate the peculiar motion of Sgr A* to be $-0.4 \pm 0.9 \text{ km s}^{-1}$ toward the north Galactic pole (see Table 3).

3.3. Acceleration of Sgr A*

The expected acceleration of the Sun in its orbit about the Galactic center currently is undetectably small: $\Theta_0^2/R_0 \approx (220 \text{ km s}^{-1})^2/8.0 \text{ kpc} \approx 6 \times 10^{-6} \text{ km s}^{-1} \text{ y}^{-1}$, or in angular units $\Theta_0^2/R_0^2 \sim 10^{-7} \text{ mas y}^{-2}$. Thus, unlike velocity measurements, which require precise knowledge and subtraction of the Sun’s orbital contribution, any measurement of acceleration can be directly attributed to Sgr A*. Since the motion of Sgr A* on the sky appears rectilinear, our data can be used to set an upper limit on any apparent acceleration of Sgr A*.

Fitting the positions listed in Table 1 to a second-order polynomial (i.e., $x = x_0 + v_x \Delta t + 0.5 a_x \Delta t^2$) allows an estimate of the acceleration. We do not detect any significant acceleration. Acceleration uncertainties (1σ) in equatorial components are $\sigma_\alpha = 0.024$, $\sigma_\delta = 0.035 \text{ mas y}^{-2}$ and in Galactic components are $\sigma_l = 0.035$, $\sigma_b = 0.026 \text{ mas y}^{-2}$. A value of 0.03 mas y^{-2} corresponds to $\approx 1 \text{ km s}^{-1} \text{ y}^{-1}$ at the distance of the Galactic center. Gould & Ramírez (1998) discuss the implications of upper limits to the acceleration of Sgr A* for the nature of Sgr A* and Galactic structure constants.

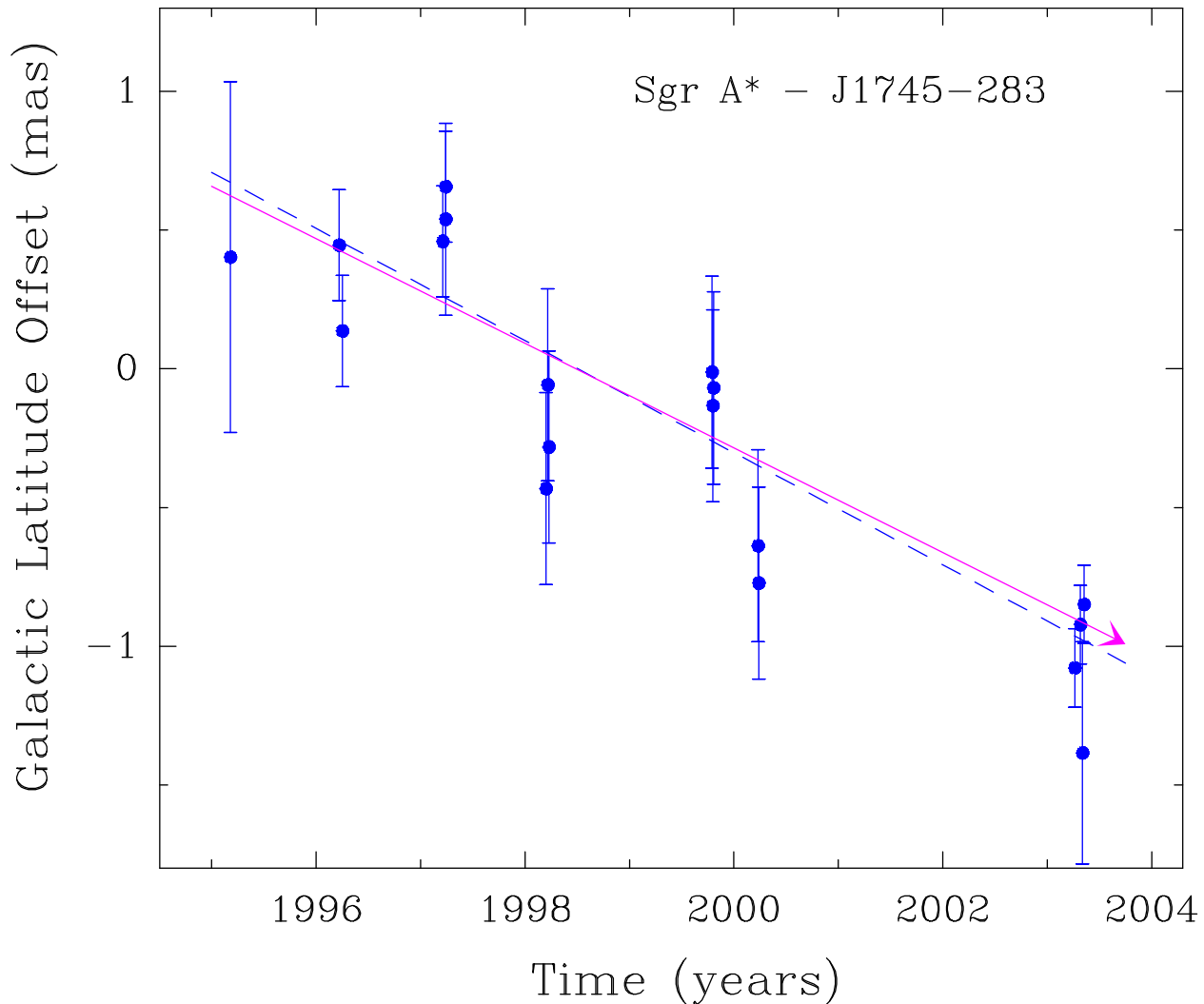


Fig. 5.— Galactic latitude position residuals of Sgr A* relative to J1745–283 from Fig. 4 on a finer scale. The dashed line is the variance-weighted best-fit proper motion of -0.202 ± 0.019 mas y^{-1} , or -7.6 ± 0.7 km s^{-1} for $R_0 = 8.0$ kpc. The solid arrow indicates the apparent motion of Sgr A* expected for the 7.17 km s^{-1} motion of the Sun perpendicular to the plane of the Galaxy. The slight tendency for data within a 1–2 week observing group to correlate suggests a small source of systemic error ($\lesssim 0.2$ mas) for data prior to 2003, probably from unmodeled atmospheric delays. Error bars are $\pm 1\sigma$ and include an estimate of this systematic uncertainty.

4. Limits on the Mass of Sgr A*

The orbits of stars as close as 100 AU from Sgr A* require a central mass of about $4 \times 10^6 M_\odot$. Our limits on the proper motion of Sgr A* can be used to indicate how much of this mass must be directly associated with Sgr A*. Since the motion of Sgr A* in the plane of the Galaxy has a much greater uncertainty (10–15 km s⁻¹, owing primarily to uncertainties in R_0 and Θ_0) than the motion out of the plane of the Galaxy (0.9 km s⁻¹), we focus mainly on the out-of-plane component. We use our strong upper limit for Sgr A*'s peculiar motion out of the plane of the Galaxy, in conjunction with 1) the constraint that $\approx 4 \times 10^6 M_\odot$ of dark matter is contained in the central 100 AU region (Schödel et al. 2003; Ghez et al. 2003), 2) the observation that Sgr A* is contained in this region (Menten et al. 1997; Reid et al. 2003), and 3) the existence of $\sim 10^6$ to 10^7 stars orbiting the galactic center within the central few parsecs (Genzel et al. 2003) to place firm lower limits to the mass directly associated with Sgr A*.

In the next sub-sections, we consider the possibility that Sgr A*'s mass does not necessarily dominate the region and compare the expected positions, velocity and acceleration of Sgr A* that might result with our observational limits. We will first consider various possibilities for configurations of the $\approx 4 \times 10^6 M_\odot$ of material known to occupy the central 100 AU region. The discussion divides along observational lines by a possible offset of Sgr A* from the dynamical center of a hypothetical dark matter distribution. Since, Sgr A* is observed to be within 100 AU of the center of this region (Schödel et al. 2003; Ghez et al. 2003; Reid et al. 2003), we do not consider offsets > 100 AU. In §4.1, we consider offsets of Sgr A* from the center of mass of the system between $4 < r < 100$ AU, where we would easily detect changes in position, but not necessarily be able to measure a velocity or acceleration, because the orbital period would be short compared to the time span of our observations used to get accurate motions. In §4.2, we consider offsets of < 4 AU, where we could detect neither a positional offset nor Sgr A*'s velocity or acceleration even though the latter two quantities could be quite large.

Following the discussion of the central 100 AU region, we calculate the effects of the $\sim 10^6$ to 10^7 stars, believed to populate the inner two parsecs of the Galactic center region, on the motion of Sgr A*. These stars orbit within the gravitational sphere of influence of Sgr A* (or more generally the $\approx 4 \times 10^6 M_\odot$ of material contained within 100 AU of the center). Even for statistically isotropic distributions of stars, random fluctuations in the mass distribution can result in a significant motion for Sgr A*. We show in §4.3 that the gravitational pull of stars in the central parsecs would induce a measurable motion for Sgr A*, were it not to contain a significant fraction of the total mass in the region. Similarly, we show in §4.4 that a compact cluster of dark stellar remnants could also induce a significant

motion for Sgr A*. Finally, in §4.5 we estimate a lower limit for the effects of stars beyond 2 pc from Sgr A* on its motion.

4.1. Sgr A* between $4 < r < 100$ AU of the Center

Were Sgr A* offset by more than 4 AU from the center of mass of the material in the inner 100 AU, we would expect to see detectable positional changes. In Fig. 6 we plot the circular orbital speeds and periods of Sgr A* for two dark matter masses: 1) where dark matter comprises essentially all of the $\approx 4 \times 10^6 M_\odot$ in the region and 2) where dark matter comprises only 10% of the mass in the region (requiring Sgr A* to contain 90% of the mass). For each case, we consider radial distributions of the dark matter that follow power-laws, and we plot three distributions of density: falling as $1/r^2$, constant in r , and rising as r^2 . It is clear from the velocity plots that, for total dark matter mass of $> 0.4 \times 10^6 M_\odot$ and physically reasonable density distributions, Sgr A* would be orbiting at very high speeds. A similar conclusion holds for Sgr A*'s acceleration.

However, the orbital periods (plotted in the lower panel of Fig. 6) would be less than 16 y for almost all models considered. Since we measure the velocity (and acceleration) of Sgr A* with data currently spanning 8 yr, we might not be sensitive to the very high velocities shown. For these cases, Sgr A*'s orbit would result in strongly-aliased, quasi-random, positional shifts with an amplitude comparable to the semi-major axis of its orbit. The residual position offsets of Sgr A* (after removing the best-fit rectilinear motion) shown in Fig. 3 are well accounted for by measurement uncertainties, which are dominated by unmodeled atmospheric propagation delays (see §2 and a more detailed discussion in Paper I). The horizontal dashed lines in Fig. 3 indicate a very conservative limit for positional “noise” from Sgr A* orbiting the center of mass in this region. Thus, components of Sgr A*'s position cannot vary by more than 2 and 4 AU in the easterly and northerly directions, and we rule out Sgr A* having an apocentric distance greater than these values. Since we have position measurements in 2-dimensions, Sgr A*'s orbital excursions are very unlikely to be hidden by projection effects.

4.2. Sgr A* within 4 AU of the Center

If Sgr A* remains within 4 AU of the dynamical center of the Galaxy, we might not detect any positional change, motion, or acceleration. Indeed this is what one would expect if Sgr A* is a SMBH containing most of the $\approx 4 \times 10^6 M_\odot$ in the central 100 AU. Could

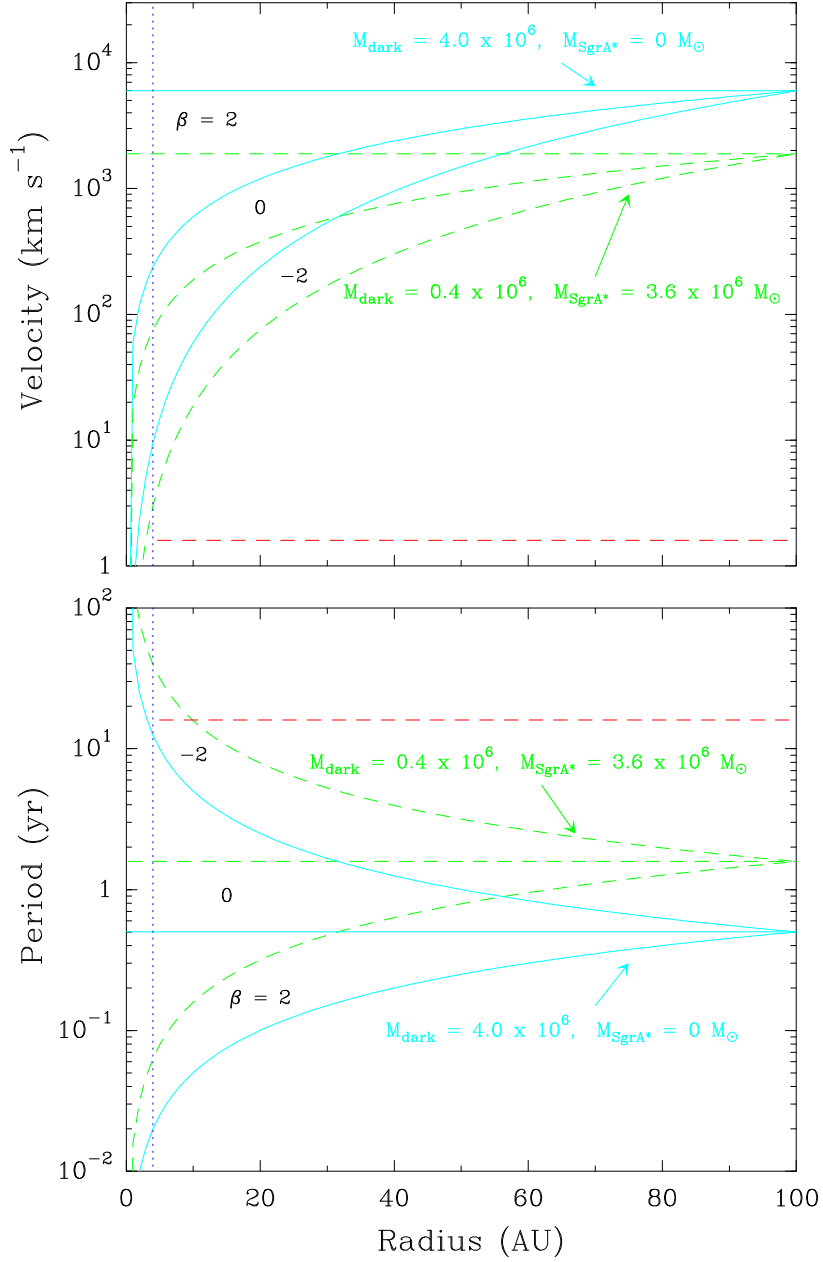


Fig. 6.— Expected velocity (*upper panel*) and orbital period (*lower panel*) of Sgr A* owing to the gravitational force of hypothetical “dark” matter distributions as a function of radius. A family of curves is plotted for each dark matter/Sgr A* mass pair: *solid lines* are dark matter dominated and *dashed lines* are Sgr A* dominated. The total mass is set to $4 \times 10^6 M_{\odot}$ in central 100 AU region, as required by observed infrared stellar orbits. For each dark matter mass, power-law distributions of density, ρ , with radius, r , given by $\rho \propto r^{-\beta}$ are plotted for $\beta = 2, 0$, & -2 . Horizontal dashed lines indicate our 2σ measurement uncertainty of 1.8 km s^{-1} for velocity and 16 y for the orbital period of Sgr A*, respectively; all values above the velocity limit would be ruled out, provided the orbital period would be longer than the period limit. Note that even though velocities of Sgr A* can be very high, orbital periods are very short and might not be detected (see §4.1). Vertical dotted lines indicate our lower limit of 4 AU for detection; for radii less than this limit greater velocities are possible. For radii greater than 4 AU position excursions for Sgr A* would be easily detected for any orbital periods.

Sgr A* be constrained to such a small region? We will see in §4.3 that the effects of stars in the central parsecs require Sgr A*, or whatever binds Sgr A* to the center, most likely to have greater than $\sim 10^6 M_\odot$. Since the binding mass must be within 4 AU of center, this requires an extraordinarily high mass density of $3 \times 10^{19} M_\odot \text{pc}^{-3}$, almost surely requiring a SMBH (see §5). Thus, by assuming that Sgr A* is not a SMBH, we cannot avoid the conclusion that a SMBH occupies the Galactic center.

Further, postulating an extremely tight binary black hole is untenable as it would decay owing to gravitational radiation on timescales of $\sim (a_{\text{AU}}^4/256f)$ y, where a_{AU} is the separation of the black holes in AUs and f is the ratio of the mass of the secondary to the total mass in the binary (Shapiro & Teukolsky 1983). Were Sgr A* only a $10 M_\odot$ object orbiting a $4 \times 10^6 M_\odot$ SMBH ($f = 2.5 \times 10^{-6}$), the time for gravitational decay from a 4 AU radius is only $\sim 4 \times 10^5$ y. Thus, Sgr A* would soon become (part of) a SMBH. Of course, the far more likely conclusion is that Sgr A* is a SMBH.

4.3. Effects of Stars Within 2 pc of Sgr A*

While we have shown that Sgr A* occupies the central 4 AU and contains enough mass to require a SMBH, it is worthwhile to investigate other constraints on Sgr A*'s motion. We now consider the effects of the orbital motions of the large number of stars observed in the central stellar cusp on Sgr A*. Random distributions of stars in orbit about Sgr A* will produce small asymmetries in the mass distribution, which vary over time and lead to small motions of Sgr A* about the center of mass of the system. In the following we first develop a simple analytic estimate of the effects of stars of a single mass in circular orbits on the motion of Sgr A*. After this we present results of detailed numerical simulations of the effects of $\sim 10^6$ to 10^7 stars in the central stellar cusp within 2 pc of Sgr A*. The numerical simulations allow us to investigate the effects of a distribution of stellar masses and orbital eccentricities.

4.3.1. Analytic Approach

We now consider the effects of bound orbital motions of a large number of stars on the motion of Sgr A*. Assume an isolated system with Sgr A* at the center of mass of a spherically symmetric random distribution of orbiting stars. Without loss of generality, we place the center of mass at the origin of a coordinate system. For this closed system, the

center of mass remains fixed and hence

$$M\vec{V} = - \sum_i m_i \vec{v}_i \quad , \quad (1)$$

where M and \vec{V} are the mass and velocity of Sgr A*, and m_i and \vec{v}_i are the mass and velocity of the i^{th} star. Squaring Eq. (1) yields

$$M^2 V^2 = \sum_i m_i^2 v_i^2 + \sum_i \sum_{j \neq i} m_i m_j \vec{v}_i \cdot \vec{v}_j \quad . \quad (2)$$

Taking expectation values for random distributions of stellar velocities, the cross terms vanish and we find

$$M^2 \langle V^2 \rangle = \sum_i \langle m_i^2 v_i^2 \rangle \quad . \quad (3)$$

For simplicity, assume a single characteristic stellar mass, m , and replace the summation in Eq. (3) with an integral:

$$\sum_i \langle m_i^2 v_i^2 \rangle = m^2 \int_r v^2(r) \left(\frac{dN}{dr} \right) dr \quad ,$$

where $\left(\frac{dN}{dr} \right) dr$ is number of stars between radii of r and $r + dr$. Eq. (3) then becomes

$$\langle V^2 \rangle = \frac{m^2}{M^2} \int_r v^2(r) \left(\frac{dN}{dr} \right) dr \quad . \quad (4)$$

For a power-law distribution of stellar mass density with radius given by $\rho(r) = \rho_0 (r/r_0)^{-\alpha}$,

$$\left(\frac{dN}{dr} \right) dr = (\rho/m) 4\pi r^2 dr = N_0 \left(\frac{r}{r_0} \right)^{2-\alpha} d(r/r_0) \quad , \quad (5)$$

where $N_0 = (\rho_0/m) 4\pi r_0^3$. For circular stellar orbits about a fixed central potential (at the average position of Sgr A*),

$$v^2(r) = \frac{GM_r}{r} \quad , \quad (6)$$

where M_r is the total mass enclosed within r , given by

$$M_r = M + \int_0^r \rho(r) 4\pi r^2 dr \quad . \quad (7)$$

Defining $\xi = r/r_0$ and $M_0 = \rho_0 4\pi r_0^3 / (3 - \alpha)$ and inserting Eqs. (5-7) into Eq. (4) yields

$$\langle V^2 \rangle = \frac{Gm^2 N_0}{Mr_0} \int_{\xi} \left(1 + \frac{M_0}{M} \xi^{3-\alpha} \right) \xi^{1-\alpha} d\xi \quad . \quad (8)$$

Integrating Eq. (8) results in

$$\langle V^2 \rangle = \frac{Gm^2 N_0}{Mr_0} \left[\frac{\xi^{2-\alpha}}{2-\alpha} + \frac{M_0}{M} \frac{\xi^{5-2\alpha}}{5-2\alpha} \right]_{\xi(r_{min})}^{\xi(r_{max})}, \quad (9)$$

for $\alpha \neq 2$ or 2.5 . (For $\alpha = 2$ or 2.5 replace the appropriate “ ξ^x/x ” terms with $\ln \xi$.)

Eq. (9) has the interesting property that it transitions smoothly from equipartition of momentum to equipartition of kinetic energy as the total mass in stars goes from that of a single star to a value equal to that of Sgr A*. This can be seen by noting that Eq. (9) can be approximated by

$$\langle V^2 \rangle \sim \frac{Gm^2 N_0}{Mr_0}, \quad (10)$$

multiplied by a dimensionless quantity of order unity. For a single star orbiting Sgr A*, $mN_0 = m$ and Eq. (10) becomes

$$M^2 \langle V^2 \rangle \sim m^2 \frac{GM}{r_0}.$$

Since the quantity GM/r_0 equals the expected square of the speed, $\langle v^2 \rangle$, of a star orbiting Sgr A* at a radius r_0 , we find equipartition of momentum:

$$M \langle V^2 \rangle^{1/2} \sim m \langle v^2 \rangle^{1/2}.$$

However, when the total stellar mass equals that of Sgr A*, $mN_0 = M$ and Eq. (10) yields equipartition of kinetic energy:

$$M \langle V^2 \rangle \sim m \langle v^2 \rangle.$$

Thus, the combined effects of bound stellar orbits result in equipartition of kinetic energy, when the total mass in stars equals the mass of the dominant central object. This resolves the problem, raised in Paper I, regarding the applicability of equipartition of kinetic energy for stellar systems bound to a massive object.

We evaluate Eq. (9) for the broken power law distribution of stars in the central cusp observed by Genzel et al. (2003): $\rho(r) = 1.2 \times 10^6 (r/0.4 \text{ pc})^{-\alpha} M_\odot \text{ pc}^{-3}$, where $\alpha = 1.4$ for $r < 0.4 \text{ pc}$ and $\alpha = 2.0$ for $r \geq 0.4 \text{ pc}$. This stellar mass distribution contains $4 \times 10^6 M_\odot$ within $r \approx 2 \text{ pc}$ of Sgr A*. We do not continue beyond this radius, as the stellar mass would start to dominate and our assumption that stars are bound to Sgr A* starts to break down. Assuming a characteristic stellar mass of $m = 0.453 M_\odot$, equal to the first moment of a standard initial mass function (Cox 2000), and Sgr A* contains $4 \times 10^6 M_\odot$, we find $\langle V^2 \rangle^{1/2} = 0.07 \text{ km s}^{-1}$, which implies individual component speeds of 0.05 km s^{-1} .

The mass function of stars in the inner two parsecs is likely to be flatter than a standard IMF, owing to mass segregation effects. Since the expected motion of Sgr A* scales as \sqrt{m} , we would expect a higher rms speed for Sgr A* than calculated above, possibly by a factor of two or more. Overall, our estimate of the motion of Sgr A* is *extremely* conservative. The assumptions of 1) a standard IMF, 2) a perfectly random stellar distribution (no clumping or anisotropies), 3) no contribution from a possible cluster of dark stellar remnants close to Sgr A* (see §4.4), and 4) no contribution from mass asymmetries beyond $r = 2$ pc (see §4.5), all contribute to give the lowest possible motion for Sgr A*.

4.3.2. Direct Simulations

The analytical approach of the previous section assumes stars of a single mass and circular orbits. In reality, one expects a distribution of stellar masses and, especially in the crowded environment of such a dense stellar system, a wide distribution of orbital eccentricities. In order to understand better the effects of stars in the central cusp on the motion of Sgr A*, we carried out full numerical simulations of the effects of the $\sim 10^6$ to 10^7 stars thought to orbit within 2 pc of the Galactic center.

We are interested in the change in position of Sgr A* over a time period of eight years. Over such a short time span (compared to typical stellar orbital periods of $\sim 10^3$ y at 0.1 pc radii), stellar motions are very short orbital arcs. Thus, there is no need to include the gravitational effects of individual stars on each other as is done in N-body calculations; we can assume that stars move along orbits determined by the mass enclosed within their semi-major axes. By avoiding full N-body calculations, we are ignoring any collective effects from stellar clumping, which would increase the expected speed of Sgr A*. So, we are being very conservative when applying the results to obtain a lower limit to the mass of Sgr A*.

We initialized a simulation by assigning each star a random stellar mass, consistent with a chosen stellar mass function. We evaluated three stellar mass functions: a standard IMF (Cox 2000), one flatter by 0.5 in the power-law indexes, and a second flatter by 1.0 in the power-law indexes. Next, we assigned each star a random semi-major axis, distributed as a broken power-law in radius as described by Genzel et al. (2003) and listed in the previous section. Orbital eccentricities were chosen from a uniform random distribution with values between 0 to 0.999. Tests with different distributions of eccentricities (eg, $dN/de \propto e$ and $dN/de \propto \sin e$ produced nearly the same results.

Each semi-major axis was initially placed on one Cartesian axis and the orbits randomized in space by three Euler rotations with angles chosen from uniform random distributions.

Note that we do not expect a significant departure from spherical symmetry within 2 pc of the Galactic center. Finally, we assigned each star a uniformly distributed initial mean anomaly.

Stars were assumed to orbit about a dominant central mass. The position of each star at time, t , was determined from its orbital elements by solving Kepler’s equations. The center of mass of the stellar cluster at time zero was determined and Sgr A* placed at that position. The position of Sgr A* at any other time could then be computed directly from the stellar masses and positions by requiring that the center of mass of the entire system remain fixed. The full velocity vector for Sgr A* was calculated by differencing positions for times separated by 8 y. In test simulations, the change of position of Sgr A* was linear, with no detectable jitter, over this time span. Over longer periods of time of order 10^4 y, Sgr A* slowly wandered by ~ 100 AU, responding to changes in the center of mass of the surrounding stars at characteristic distances of 1 pc. (This is unlikely to affect measurements of stellar orbits for stars within ≈ 0.01 pc, as these stars are tightly bound to Sgr A* and should wander with it.)

We computed 1000 simulations of the effects of $\sim 10^6$ to 10^7 stars on the motion of Sgr A* for the three stellar mass functions (discussed above). For a standard initial mass function (IMF) and a mass of Sgr A* of $4 \times 10^6 M_\odot$, the root-mean-square speed for Sgr A* was 0.17 km s^{-1} and each component of the velocity vector was 0.10 km s^{-1} . This single component speed is a factor of two greater than the 0.05 km s^{-1} value obtained by the analytic treatment in §4.3.1. However, as pointed out earlier, that treatment assumed circular orbits and a single (average) stellar mass. We tested our numerical simulation under these restrictive conditions ($e = 0$ and $m = 0.453 M_\odot$, corresponding to the first mass moment of a standard IMF) and obtained 0.05 km s^{-1} for a single component speed of Sgr A*, in agreement with the analytical result.

In order to determine a lower limit to the mass of Sgr A*, given our 0.9 km s^{-1} (1σ) measurement uncertainty in the component of Sgr A*’s velocity out of the plane of the Galaxy, we estimate the motion of Sgr A* as a function of its mass. As shown in §4.3.1, equipartition of kinetic energy holds when the total mass in stars equals that of Sgr A*. Thus, the expected motion of Sgr A* (V_z) should scale as $1/\sqrt{M}$, with one possible caveat. For cases where $M \ll 4 \times 10^6 M_\odot$, it would be important to replace the “missing mass” in order to satisfy the central mass constraints from infrared stellar orbits. Not doing this might violate the assumption in our calculations that Sgr A* is perturbed only by the observed central stellar cluster. One could correct for this with full N-body calculations, provided one knew the nature of this hypothetical “missing dark matter.” However, this is not known. Note that if dark matter (other than a SMBH) dominates in the central 100 AU region, then,

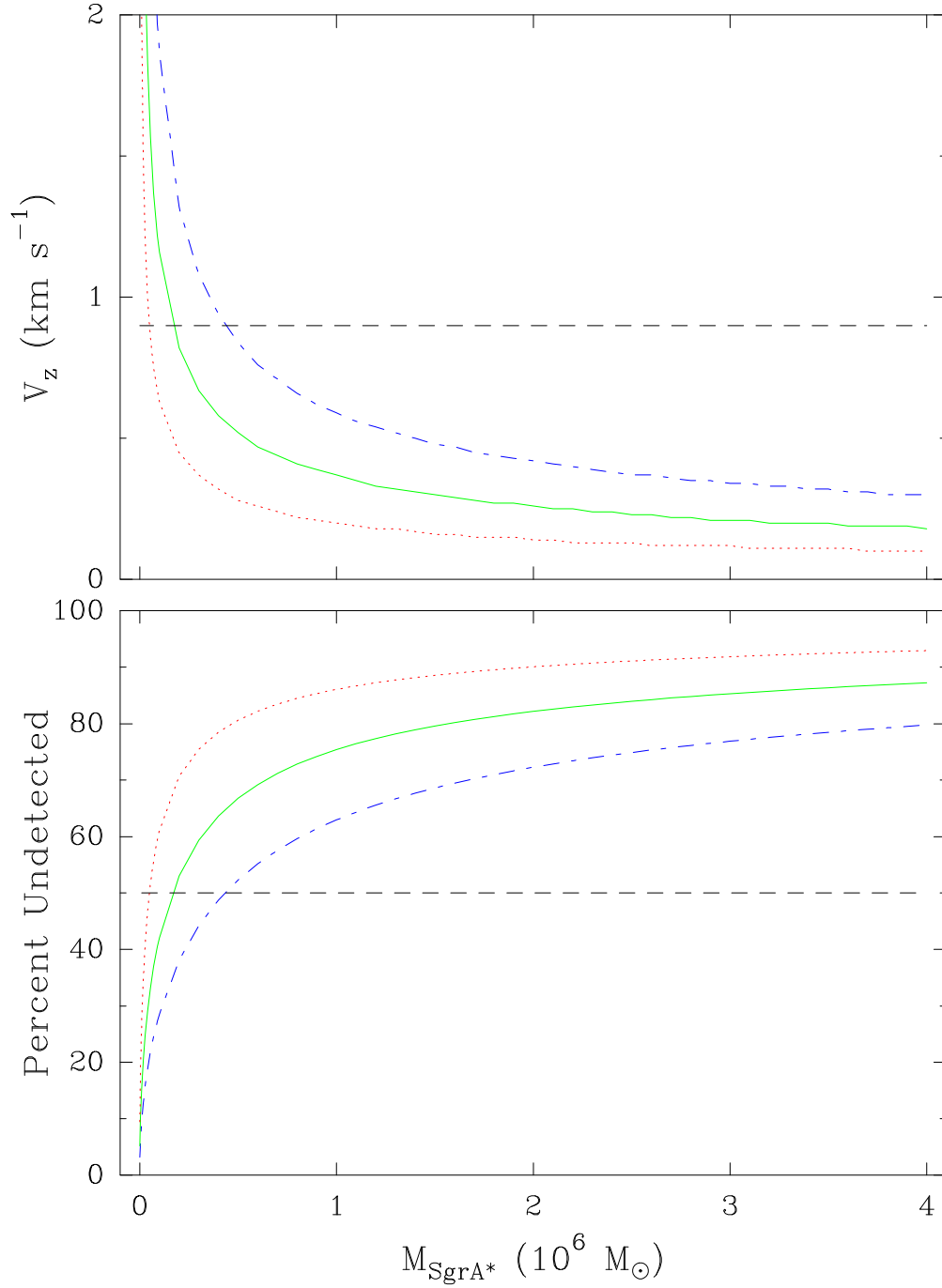


Fig. 7.— Results of direct simulations of the motion of Sgr A*, owing to the gravitational forces of stars in random orbits within 2 pc of the Galactic center. Three simulations for different stellar initial mass functions (IMF) are plotted: the *dotted* line corresponds to a standard IMF, and the *solid*, and *dot-dashed* lines correspond to mass functions flatter by 0.5 and 1.0 in their power-law indexes. A flatter than standard IMF is expected owing to mass segregation from dynamical friction and observed in the Arches Galactic center cluster. *Upper panel*: The simulated root-mean-square of one component of the velocity of Sgr A* as a function of its mass. The *dashed line* indicates our 1σ measurement uncertainty of 0.9 km s^{-1} . *Lower panel*: The percent of simulations where the motion of Sgr A* is less than a trial measurement, with the *dashed line* indicating the 50% or maximum likelihood limit.

as discussed in §4.1, Sgr A* must still be bound within 4 AU of center.

The motion of Sgr A* as a function of its mass is shown in Fig. 7. The upper panel gives the rms speed for one component of Sgr A*'s motion. The three curves correspond to three different stellar mass functions. While we do not know the stellar mass function of the Galactic center cluster, it is observed to contain an unusually large population of very massive stars (Krabbe, Genzel, Drapatz, & Rotaciuc 1991; Najarro et al. 1997). This may result from the unusual physical conditions in the Galactic center, which might favor high mass star formation (Morris 1993). Also, the Galactic center cluster is very likely to have undergone significant mass segregation, with more massive stars “sinking” closer to the center than less massive stars, owing to the effects of dynamical friction. Observationally, the Arches cluster near the Galactic Center has a mass spectrum index flatter by about +0.6 to +0.8 than other Galactic clusters (Figer et al. 1999; Stolte, Grebel, Brandner, & Figer 2002) or a standard IMF. Because of these findings, we feel the best estimate of Sgr A*'s expected motion is between the curves for stellar mass function whose indexes are flatter than for a standard IMF by 0.5 to 1.0. Thus, if Sgr A* contains $4 \times 10^6 M_{\odot}$, we expect it to have a motion in one-dimension of between 0.18 and 0.30 km s⁻¹, respectively. Decreasing the mass of Sgr A* would increase its expected speed as shown in Fig. 7.

We now proceed to estimate a maximum-likelihood lower limit to the mass of Sgr A*, by calculating the percent of stellar cluster simulations for which a velocity component of Sgr A*'s motion would be less than a measurement drawn from a Gaussian random distribution with $\sigma_m = 0.9$ km s⁻¹, matching our observational accuracy. For any given measurement of the 1-dimension velocity of Sgr A*, V_m , the fraction of the simulations that would have a lower speed is given by

$$\text{Erf}(V_m, \sigma_s) = \frac{1}{\sigma_s \sqrt{2\pi}} \int_{-V_m}^{-V_m} e^{-V^2/2\sigma_s^2} dV \quad ,$$

where σ_s is the root-mean-square of the simulated (1-D) velocities of Sgr A*. For a Gaussian distribution of measurements, V_m , the probability of measuring a value between V_m and $V_m + dV$ is given by,

$$G(V_m, \sigma_m) dV_m = \frac{1}{\sigma_m \sqrt{2\pi}} e^{-V_m^2/2\sigma_m^2} dV_m \quad .$$

Then the probability, $P(\sigma_s, \sigma_m)$, that we would not detect a simulation of Sgr A*'s motion with a given measurement (i.e., $|V_s| < |V_m|$) is given by

$$P(\sigma_s, \sigma_m) = \int_{-\infty}^{\infty} \text{Erf}(V, \sigma_s) G(V, \sigma_m) dV \quad . \quad (11)$$

In the lower panel of Fig. 7 we plot $P(\sigma_s, \sigma_m)$ as a function of the mass of Sgr A* for the three stellar mass functions. We find that simulated motions of Sgr A* would exceed measurements 50% of the time for Sgr A* masses of 0.05, 0.2, and $0.5 \times 10^6 M_\odot$ for a standard IMF, and stellar mass function indexes flatter by 0.5 and 1.0, respectively. These mass estimates are maximum-likelihood lower limits to the mass of Sgr A*. Because the stellar mass function is likely considerably flatter than a standard IMF (see discussion above), we adopt a lower limit to the mass of Sgr A* of $0.4 \times 10^6 M_\odot$, a value between those for the two flatter stellar mass functions.

As discussed in §3, the component of the motion of Sgr A* in the plane of the Galaxy (in the direction of Galactic rotation) is much less well determined than the component out of the plane. Because we can effectively use only one component of the velocity vector to limit the mass of Sgr A*, there is non-negligible possibility that projection effects could hide a more significant motion. An examination of Fig. 7 reveals that, as one demands higher confidence for the percentage of cases for which we would not detect a motion of Sgr A*, the mass limit decreases rapidly. For example, for a 95% confidence limit (< 5% undetected in Fig. 7), the mass limit is $\sim 10^3 M_\odot$. However, reducing the mass of Sgr A* well below $\sim 10^6 M_\odot$ opens the question of how to satisfy the constraint from stellar orbits that $4 \times 10^6 M_\odot$ is contained in the central 100 AU. Replacing most of the mass in the central 100 AU with dark matter (Bilić, Munyaneza, Tupper, & Viollier 2002) or stellar remnants may already be ruled out (Maoz 1998; Ghez et al. 2003; Schödel et al. 2003). Because of these difficulties, as well as the extremely conservative assumptions used to calculate the motion of Sgr A*, we adopt the maximum likelihood estimate of $0.4 \times 10^6 M_\odot$ for the lower limit to the mass of Sgr A*.

4.4. Effects of a Central Dark Stellar Cluster

In addition to a visible stellar cluster, the center of the Galaxy may contain large numbers of dark stellar remnants. Mouawad et al. (2004) suggest that the infrared positional data for star S2 support a model with a SMBH of $3.7 \times 10^6 M_\odot$, plus a compact dark cluster with a mass of $0.4 \times 10^6 M_\odot$. Such a compact dark cluster might be composed of massive stellar remnants which migrated toward the Galactic center over billions of years owing to dynamical friction. If such a dark cluster exists, it would also affect the motion of Sgr A*.

In order to quantify the motion of Sgr A* under the influence of a compact cluster of stellar remnants, we modified the computer code used in the previous section to simulate this case. Instead of power-law radial distributions, we adopted Plummer distributions following Mouawad et al. (2004). We considered dark clusters of stellar remnants totaling $0.4 \times 10^6 M_\odot$, containing 50% neutron stars of $1.4 M_\odot$ and 50% black holes with a uniform distribution of

mass between 3 and 25 M_{\odot} . The core radius of the cluster was varied and large numbers of random simulations were evaluated to determine the rms velocity of a $3.6 \times 10^6 M_{\odot}$ Sgr A*. As before, we calculated the position of Sgr A* at times separated by 8 years and differenced these to determine a velocity in order to mimic our observations.

The results of our simulations are shown in Fig. 8. A cluster of only $\sim 5 \times 10^4$ dark stellar remnants containing $0.4 \times 10^6 M_{\odot}$ could contribute $> 0.3 \text{ km s}^{-1}$ to one component of the measured motion of Sgr A*. Mouawad et al. (2004) find a best-fit core radius of 0.0155 pc, which would give a $3.6 \times 10^6 M_{\odot}$ Sgr A* a 1-dimensional rms motion of 0.34 km s^{-1} . Furthermore, over a wide range of core radii from about 0.004 to 0.4 pc, such a cluster could contribute about $> 0.2 \text{ km s}^{-1}$. Thus, a contribution to the motion of Sgr A* from a cluster of dark stellar remnants might be comparable to the contribution of the $\sim 10^6$ to 10^7 stars observed within 2 pc of Sgr A*. Were we to add a contribution from such a cluster of dark stellar remnants ($\approx 0.3 \text{ km s}^{-1}$) to the motion of Sgr A* from the calculations in §4.3 ($\approx 0.2 - 0.3 \text{ km s}^{-1}$), the quadrature sum for the 1-dimensional motion of Sgr A* would be $\approx 0.4 - 0.5 \text{ km s}^{-1}$. This would increase the lower limit of the mass of Sgr A* to 0.7 or $1.7 \times 10^6 M_{\odot}$ for the two flatter mass functions considered above.

4.5. Effects of Stars Beyond 2 pc

The large number of stars (as well as a significant amount of dust and gas) at radial distances greater than 2 pc from Sgr A* must also contribute to the motion of Sgr A*. However, since the total mass of such material can greatly exceed that of Sgr A*, we cannot use the methods of §4.3, which require the stars to reside in the gravitational sphere of influence of Sgr A*. In general, this problem requires very large N-body calculations. Recently, Chatterjee, Hernquist, & Loeb (2002) and Dorband, Hemsendorf & Merritt (2003) addressed this theoretically as a Brownian motion problem and by N-body simulations. Both papers conclude that the “Brownian particle,” Sgr A*, would come into equilibrium rapidly with the sea of surrounding stars and achieve equipartition of kinetic energy.

For equipartition of kinetic energy,

$$M \langle V^2 \rangle \approx m \langle v^2 \rangle, \quad (12)$$

where capital and lower case symbols refer to Sgr A* and a typical star, respectively. The characteristic speed of a star is given by $\langle v^2 \rangle \approx GM_r/r$, where M_r is defined in Eq. (7). If the stellar density is given by $\rho = \rho_0(r/r_0)^{-2}$, then $M_r = M + \rho_0 4\pi r_0^2 r$. At a sufficiently large radius such that stars dominate the enclosed mass, M_r/r approaches a constant and

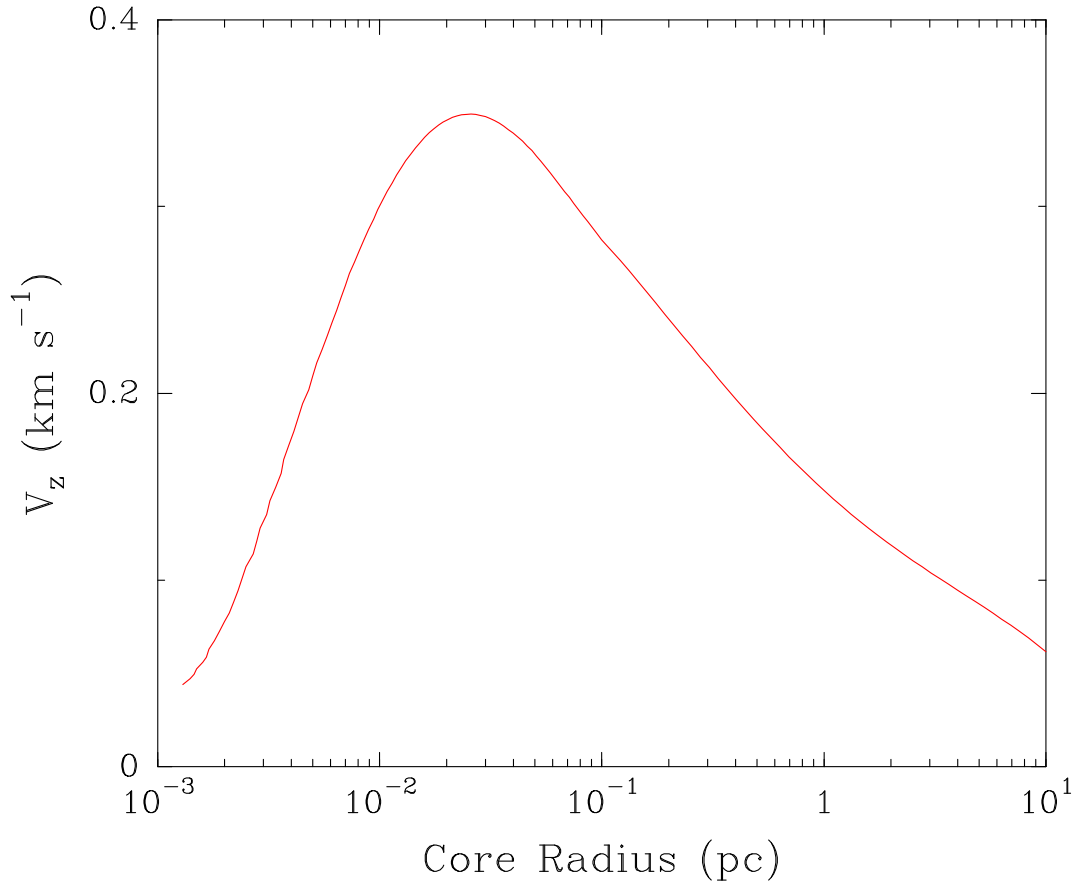


Fig. 8.— Results of direct simulations of the motion of Sgr A*, owing to the gravitational forces of random stellar orbits, for a hypothetical cluster of stellar remnants. The stellar cluster was assumed to contain $0.4 \times 10^6 M_{\odot}$ with Plummer radial distribution. The line traces the simulated root-mean-square of one component of the velocity of Sgr A* as a function of the core radius of the Plummer distribution. For core radii less than about 0.03 pc, the velocity obtained by fitting a straight line to positions over an 8 year period, similar to our observations, is smaller than the instantaneous velocity owing rapid fluctuations in position caused by stellar remnants with orbital periods < 16 y.

$\langle v^2 \rangle \approx G\rho_0 4\pi r_0^2$. For this case, Eq. (12) yields

$$\langle V^2 \rangle \approx \frac{m}{M} G\rho_0 4\pi r_0^2 \quad , \quad (13)$$

independent of radius. As before, adopting the Genzel et al. (2003) model for the radial distribution of stars with $r > 0.4$ pc, $\rho(r) = 1.2 \times 10^6 (r/0.4 \text{ pc})^{-2} \text{ M}_\odot \text{ pc}^{-3}$, Eq. (13) indicates that distant stars with $m \approx 1 \text{ M}_\odot$ should contribute to the motion of a $4 \times 10^6 \text{ M}_\odot$ black hole as $\langle V^2 \rangle^{1/2} \approx 0.05 \text{ km s}^{-1}$. This speed should be considered a lower limit, since any asymmetries caused, for example, by clustering of stars would increase the expected motion of Sgr A*, as would inclusion of a expected stellar mass function. Also, as pointed out by Backer & Sramek (1999), the possibility of large scale asymmetries in not only the stellar distribution, but also from massive molecular clouds, could significantly increase the motion of Sgr A*. Note, however, that very large scale asymmetries (eg, > 100 pc from the center) would most likely be confined to the plane of the Galaxy and may not affect the out-of-plane motion of Sgr A*.

5. Is Sgr A* a Super-Massive Black Hole

Based on the results discussed in §4, we conclude that the compact radio source, Sgr A*, contains at least 10% of the $4 \times 10^6 \text{ M}_\odot$ in the inner 100 AU region. The apparent size of Sgr A* measured with VLBI techniques is dominated by scatter broadening, and its intrinsic size is less than about 1 AU (Rogers et al. 1994; Krichbaum et al. 1998; Doeleman et al. 2001; Bower et al. 2004). Thus, we require a mass of $> 0.4 \times 10^6 \text{ M}_\odot$ within a radius of < 0.5 AU, which yields an astounding mass density of $> 7 \times 10^{21} \text{ M}_\odot \text{ pc}^{-3}$.

In making the density calculation, we have assumed that the size of the emitting region is equal to or greater than the size of the region containing the mass. This is true for almost all astrophysical sources. Notable exceptions for radio sources are solar flares and pulsars. However these sources are sporadic (either flares or pulses) and are usually characterized by gyro-synchrotron emission with very steep spectral indexes. Sgr A* does not share these characteristics, especially in the radio band where its emission is dominated by a generally slowly varying, smooth, rising spectrum. Thus, we conclude that our assumption that the radiative size of Sgr A* equals or exceeds the physical size is reasonable.

Table 4 lists the mass densities of notable super-massive black hole candidates. The mass density we have determined for Sgr A* is six orders of magnitude higher than can be determined currently from infrared stellar orbits. It is 12 orders of magnitude greater than for NGC 4258 (from imaging an 0.1 pc radius accretion disk through its H₂O maser emission) and nearly 17 orders of magnitude greater than for M 87 (from HST spectroscopy

of a central stellar cluster). Our mass density is within about three orders of magnitude of that for a $4 \times 10^6 M_\odot$ black hole within its Schwarzschild radius, R_{Sch} . If one adopts a minimum possible radius of $3R_{\text{Sch}}$ for a stable object, then the lower limit for the mass density of Sgr A* is within only two orders of magnitude of the super-massive black hole value. Thus, the mass density determined from the proper motion limit for Sgr A*, coupled with its very small intrinsic size, is the strongest and most direct evidence to date that the compact radio source, Sgr A*, is a super-massive black hole.

6. Limits on a Binary Black Hole

The possibility that a binary black hole exists in the center of the Galaxy has been discussed by Hansen & Milosavljević (2003) and Yu & Tremaine (2003). Such a binary could arise as a dense stellar cluster, containing an intermediate mass black hole, is dragged toward a more massive black hole (Sgr A*) at the center of the Galaxy. This scenario is interesting as it might help to explain the existence of large numbers of massive young stars in the central stellar cluster, which are unlikely to have formed at their present locations.

As suggested by Hansen & Milosavljević (2003), limits on the orbital excursion and velocity of Sgr A* provide strong constraints on the masses and semi-major axes of secondary (intermediate mass) black holes in the Galactic center region. Our current observations support limits between those plotted by Hansen & Milosavljević (2003) in their Fig. 2 for “astrometric resolutions” of 0.1 and 1.0 mas. The limits on these parameters are complex and depend on both parameters, but roughly we can exclude secondary black holes with masses greater than $\sim 10^4 M_\odot$ and semi-major axes between 10^3 and 10^5 AU from Sgr A*. Excluding stellar mass black holes ($< 100 M_\odot$) will require more than an order of magnitude better astrometric accuracy and is unlikely in the near future.

7. Conclusions

We have measured the position of the compact non-thermal radio source, Sgr A*, at the center of the Galaxy relative to extragalactic radio sources. The apparent motion of Sgr A* is consistent with that expected from the orbit of the Sun around the Galactic center. Any peculiar motion of Sgr A* perpendicular to the plane of the Galaxy is less than 1.8 km s^{-1} (2σ). This result is complementary to infrared observations of stellar orbits at the Galactic center, which require $4 \times 10^6 M_\odot$ within a radius of 100 AU of Sgr A*. The results of several different analyses indicate a significant fraction, if not all, of the mass in the central 100 AU

is tied to Sgr A*. Were Sgr A* not a SMBH, it must be bound to the inner 4 AU of the dynamical center of the Galaxy. This would imply an extraordinarily high mass density and probably require a SMBH.

The gravitational attractions of the $\sim 10^6$ to 10^7 stars within 2 pc of the Galactic center impart a significant motion to Sgr A*. Based on numerical simulations of the central star cluster and our upper limit to the motion of Sgr A* out of the plane of the Galaxy, a maximum-likelihood lower limit for the mass of Sgr A* is $0.4 \times 10^6 M_\odot$. These analyses make very conservative assumptions that would tend to underestimate the motion of Sgr A* and, hence, underestimate the mass limit. This is the first *direct* evidence that a compact radiative source at the center of a galaxy is a super-massive object. Other measurements determine a large mass, but can only *indirectly* associate it with the radiative source through positional agreement.

The observed radio frequency size of Sgr A* is less than 1 AU, after accounting for the effects of interstellar scattering. The mass density implied by having at least $0.4 \times 10^6 M_\odot$ within a 0.5 AU radius is a staggering $7 \times 10^{21} M_\odot \text{ pc}^{-3}$! This is only about 3 orders-of-magnitude lower than the mass density of a $4 \times 10^6 M_\odot$ black hole within its Schwarzschild radius, providing overwhelming evidence that Sgr A* is a super-massive black hole. Should future VLBI measurements at 1 mm wavelength show that the intrinsic size of Sgr A* is ≈ 0.2 AU, then we could conclude that most of the mass in the region required for a super-massive black hole is contained within a few R_{Sch} for Sgr A*.

We thank V. Dhawan for helping with the VLBA setup, A. Loeb and F. Rasio for discussions that led to the analysis presented in §4.3.1, and J. Goodman and R. Narayan for discussions on the characteristics of the probability distribution for the mass limit for Sgr A* using only one component of its motion.

A. Appendix

The IAU Galactic plane (Blaauw et al. 1960) is defined in B1950 coordinates by a north Galactic pole toward $\alpha_p^{1950} \equiv 12^{\text{h}} 49^{\text{m}}, \delta_p^{1950} \equiv +27.4^\circ$ and the “zero of longitude is the great semi-circle originating at the new north galactic pole at the position angle $\theta^{1950} \equiv 123^\circ$.” This gives a B1950 origin for galactic coordinates of $\alpha_0^{1950} = 17^{\text{h}} 42^{\text{m}} 26.603^{\text{s}}, \delta_0^{1950} = -28^\circ 55' 00.445''$ (Lane 1979). Converting the B1950 coordinates to J2000 coordinates, we obtain $\alpha_p^{2000} = 12^{\text{h}} 51^{\text{m}} 26.282^{\text{s}}, \delta_p^{2000} = +27^\circ 07' 42.01''$ and $\alpha_0^{2000} = 17^{\text{h}} 45^{\text{m}} 37.224^{\text{s}}, \delta_0^{2000} = -28^\circ 56' 10.23''$. In order to carry the IAU definition of the Galactic plane forward to J2000 coordinates, we need to determine a new value of θ . We do this by requiring that the J2000

coordinates of the origin gives zero longitude, which yields $\theta^{2000} = 122.932^\circ$. Note that at the position of the Galactic center, the projection of the Galactic plane is at a position angle of 31.72° and 31.40° east of north in B1950 and J2000 coordinates, respectively. Blaauw et al. (1960) suggest a probable error of ± 0.1 degrees in the orientation of the Galactic pole, and hence the Galactic plane.

REFERENCES

- Backer, D. C. & Sramek, R. A. 1999, *ApJ*, 524, 805
- Bilic, N., Munyaneza, F., Tupper, G. B., & Viollier, R. D. 2002, *Progress in Particle and Nuclear Physics*, 48, 291
- Blaauw, A., Gum, C. S., Pawsay, J. L. & Westerhout, G. 1960, *MNRAS*, 121, 123
- Bower, G. C., Backer, D. C., & Sramek, R. A. 2001, *ApJ*, 558, 127
- Bower, G. et al. 2004, submitted to *Science*
- Chatterjee, P., Hernquist, L., & Loeb, A. 2002, *ApJ*, 572, 371
- Cox, A. N., 2000, “Allen’s Astrophysical Quantities,” (AIP Press/Springer-Verlag, New York)
- Dehnen, W. & Binney, J. J. 1998, *MNRAS*, 298, 387
- Doeleman, S. S. et al. 2001, *AJ*, 121, 2610
- Dorband, E. N., Hemsendorf, M. & Merritt, D. 2003, *J. Comp. Phys.*, 185, 484
- Eisenhauer, F., Schödel, R., Genzel, R., Ott, T., Tecza, M, Abuter, R., Eckart, A., & Alexander, T. 2003, *ApJ*, 597, L121
- Feast, M. & Whitelock, P. 1997, *MNRAS*, 291, 683
- Figer, D. F., Kim, S. S., Morris, M., Serabyn, E., Rich, R. M., & McLean, I. S. 1999, *ApJ*, 525, 750
- Ford, H. C., et al. 1994, *ApJ*, 435, L27
- Genzel, R. et al. 2003, *ApJ*, 594, 812
- Ghez, A. M. et al. 2003, *ApJ*, 586, L127

- Gould, A. & Ramírez, S. V. 1998, *ApJ*, 497, 713
- Hansen, B. M. S. & Milosavljević, M. 2003, *ApJ*, 593, L77
- Harms, R. J., et al. 1994, *ApJ*, 435, L35
- Hosokawa, M., Jauncey, D., Reynolds, J., Tzioumis, A., Ohnishi, K. & Fukushima, T. 2002, *ApJ*, 580, L43
- Kerr, F. J. & Lynden-Bell, D. 1986, *MNRAS*, 221, 1023
- Kalirai, J. S., et al. 2004, *ApJ*, 601, 277
- Krabbe, A., Genzel, R., Drapatz, S., & Rotaciuc, V. 1991, *ApJ*, 382, L19
- Krichbaum, T. P. et al. 1998, *A&A*, 335, L106
- Ma, C. et al. 1998, *AJ*, 116, 516
- Maoz, E. 1998, *ApJ*, 494, L181
- Menten, K. M., Reid, M. J., Eckart, A. & Genzel, R. 1997, *ApJ*, 475, L111
- Miyoshi, M., Moran, J., Herrnstein, J., Greenhill, L., Nakai, N., Diamond, P., & Inoue, M. 1995, *Nature*, 373, 127
- Morris, M. 1993, *ApJ*, 408, 496
- Mouawad, N., Eckart, A., Pfalzner, S., Schödel, R., Moulataka, J. & Spurzem, R. 2004, *Astro-ph/0402338*
- Najarro, F., Krabbe, A., Genzel, R., Lutz, D., Kudritzki, R. P., & Hillier, D. J. 1997, *A&A*, 325, 700
- Reid, M. J. 1993, *ARA&A*, 31, 345
- Reid, M. J., Readhead, A. C. S., Vermeulen, R. C., & Treuhaft, R. N. 1999, *ApJ*, 524, 816
- Reid, M. J., Menten, K. M., Genzel, R., Ott, T., Schödel, R., & Eckart, A. 2003, *ApJ*, 587, 208
- Rogers, A. E. E. et al. 1994, *ApJ*, 434, L59
- Schödel, R. et al. 2002, *Nature*, 419, 694

Schödel, R., Ott, T., Genzel, R., Eckart, A., Mouawad, N., & Alexander, T. 2003, *ApJ*, 596, 1015

Serabyn, E., Carlstrom, J., Lay, O., Lis, D. C., Hunter, T. R., Lacy, J. H. & Hills, R. E. 1997, *ApJ*, 490, L77

Shapiro, S. L. & Teukolsky, S. A. 1983, “Black Holes, White Dwarfs, and Neutron Stars: The Physics of Compact Objects,” (Wiley-Interscience Pub., New York), p. 477

Stolte, A., Grebel, E. K., Brandner, W., & Figer, D. F. 2002, *A&A*, 394, 459

Yu, Q. & Tremaine, S. 2003, *ApJ*, 599, 1129

Walker, R. C. 2000, International VLBI Service for Geodesy and Astrometry: 2000 General Meeting Proceedings, p. 42, 42

Table 4. Mass Densities of SMBH Candidates

Source	Density ($M_{\odot} \text{ pc}^{-3}$)	Mass (M_{\odot})	Radius	References
M 87	1×10^5	2×10^9	18 pc	1
NGC 4258 ...	7×10^9	3×10^7	0.1 pc	2
Sgr A*	$> 8 \times 10^{15}$	4×10^6	$< 100 \text{ AU}$	3
Sgr A*	$> 7 \times 10^{21}$	$> 4 \times 10^5$	$< 0.5 \text{ AU}$	4
SMBH	2×10^{25}	4×10^6	0.08 AU	

¹Ford et al. (1994); Harms et al. (1994)

²Miyoshi et al. (1995)

³Schödel et al. (2003); Ghez et al. (2003)

⁴Mass limit from this paper; Size limit from Rogers et al. (1994); Krichbaum et al. (1998); Doeleman et al. (2001); Bower et al. (2004)